
CP2Image: Generating high-quality single-cell images using CellProfiler representations

Yanni Ji¹, Marie F.A. Cutiongco², Bjørn Sand Jensen^{3,1} and Ke Yuan¹

¹ School of Computing Science, University of Glasgow.

² Nanyang Technological University

³ Technical University of Denmark, Department of Applied Mathematics and Computer Science.

{2301589j@student.gla.ac.edu, Marie.Cutiongco@ntu.edu.sg,
bjje@dtu.dk, Ke.Yuan@glasgow.ac.uk}

Abstract

Single-cell high-throughput microscopy images contain key biological information underlying normal and pathological cellular processes. Image-based analysis and profiling are powerful and promising for extracting this information but are made difficult due to substantial complexity and heterogeneity in cellular phenotype. Hand-crafted methods and machine learning models are popular ways to extract cell image information. Representations extracted via machine learning models, which often exhibit good reconstruction performance, lack biological interpretability. Hand-crafted representations, on the contrary, have clear biological meanings and thus are interpretable. Whether these hand-crafted representations can also generate realistic images is not clear. In this paper, we propose a CellProfiler to image (CP2Image) model that can directly generate realistic cell images from CellProfiler representations. We also demonstrate most biological information encoded in the CellProfiler representations is well-preserved in the generating process. This is the first time hand-crafted representations be shown to have generative ability and provide researchers with an intuitive way for their further analysis.

1 Introduction

With the advance in high-throughput microscopy, researchers can efficiently acquire a large number of cell images under a variety of conditions [20]. These images contain rich biological information on cell lineage, biomolecular pathway activation, and morphological cell characteristics, encouraging discoveries focused on visual manifestations of cellular state [13].

Several approaches exist to either implicitly or explicitly capture or characterize the morphology of cells [8, 9, 18, 19]. Traditionally, cell morphology has been quantified and investigated through the use of hand-crafted features such as CellProfiler (CP) [3] or EBImage; however, machine learning approaches have recently shown that it is possible to learn useful representations of cell morphology [4] for image generation, phenotype characterization, and downstream prediction tasks [7]. Learned representation often results in impressive performance when generating images of cells [4, 7] or discriminating, for example, the mechanism of action (MoA); however, the learned representations (i.e., internal/latent states in a neural network model) are often difficult to understand from a biological perspective as they lack clear linkage with the known biological phenomenon. The use of machine learning for learning representation of cells is therefore partly hindered by the lack of interpretability when it comes to the model’s internal, quantitative representation of the cell morphology. On the other hand, many of the machine learning models are so-called generative models with the advantage that they allow scientists an intuitive visual understanding of the representation, thus improving the interpretability of the learned model for non-experts.

Prior work has shown that CP representations contain discriminative information about drug effects and functions, such as the MoA. Hence if we know or make changes to CP representations associated with a specific drug, it would be valuable to visualize the expected effects on cells, thereby facilitating a better understanding of the counterfactuals, out-of-distribution samples, and the overall causal structure between drugs and effects on cells. Furthermore, in rare cases, researchers only have access to CP representations without the corresponding images, thus leaving no opportunity for visual comparison across experiments.

In this work, we propose a new model (CP2Image) that uses CP representations to generate photorealistic images of cells. CP2Image consists of a convolutional neural network-based generator, which takes CP representations as input, and outputs cell images. The model leverages a discriminator network, similar to the VAEplus model [7], to enhance the image quality. We show that our model generates high-quality cell images from the CP representations. Measured by the Fréchet inception distance (FID) score, our model outperforms the state-of-the-art variational autoencoder VAE [6]. We also demonstrate how changing the values of input CP representations, such as nuclei-related dimensions, results in corresponding effects in the generated images. We believe this is the first successful attempt at generating photo-realistic single-cell images solely from CP representations.

2 The CP2Image model

To investigate whether interpretable CP representations can be used to generate cell images, we propose a convolutional neural network model shown in Figure 1. The input is a CP representation $z \in \mathbb{R}^p$, where p is the dimension of a CP feature vector. The output is the generated image $X_{gen} \in \mathbb{R}^{d \times d \times 3}$, where d is the image size. The model consists of four blocks, and each block contains a convolutional layer, a leaky ReLU layer, and an upsampling layer. Batch normalisation layers are used throughout the model. To enhance the generative performance, we add a GAN-style discriminator as the second component. The discriminator consists of five blocks, and each block contains a convolutional layer, a leaky layer and a pooling layer. Batch normalisation layers is used throughout the network. The loss function is calculated using the mean squared error (MSE) loss of generated image X_{gen} and corresponding original image $X_{orig} \in \mathbb{R}^{d \times d \times 3}$.

We first fed the original images and generated images to the discriminator. For each layer i , we extracted the hidden representation for that layer and calculated the MSE loss between original and generated images at that layer, which is denoted as \mathcal{L}_i^H . We added up the layers, defined as $\mathcal{L}^H = \sum_i \gamma_i \mathcal{L}_i^H$. This loss encourages the generated images to be similar to the original images at all stages of the process.

Then we fed another real image batch $X_{real} \in \mathbb{R}^{d \times d \times 3}$ into the discriminator D , where X_{real} is independent from X_{orig} . For real images and generated images, we calculated the cross entropy loss which is used to train the discriminator to classify the real and generated images.

$$\mathcal{L}^{Dis} = -\log D(X_{real}) - \log(1 - D(X_{gen}))$$

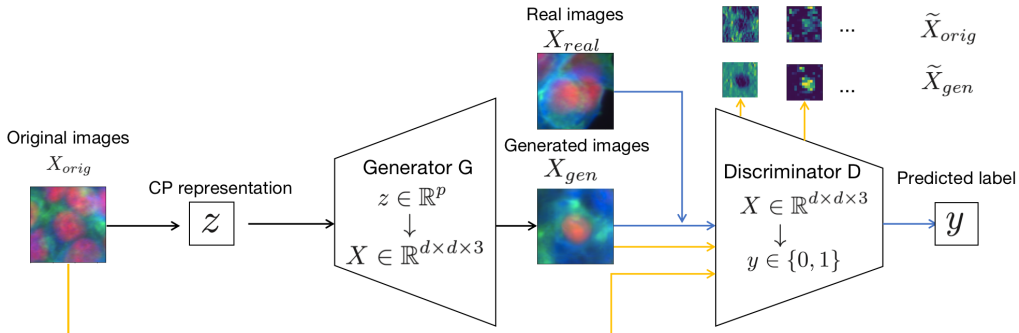


Figure 1: CP2Image model consists of two parts: a generator that generates images from CP representations, and a discriminator to enhance generation performance. The yellow line represents original and generated images feeding into the discriminator for hidden representations MSE loss. The blue line shows the real and generated images feeding into the discriminator for discriminator loss. The model architecture is adapted from VAEplus [7].

We alternate the training between the generator and discriminator during every iteration. When training the generator, we optimize the objective $\mathcal{L}^{MSE} + \mathcal{L}^H$. When training the discriminator, we optimize the objective \mathcal{L}^{Dis} . To stabilize the discriminator training, we added spectral normalization [11] in the discriminator network.

3 Experiment and results

3.1 Experiment

We use the benchmark BBBC021 dataset, which has been used for capturing cell responses to drugs in previous research [7, 10, 16, 12, 1, 5, 2, 15, 14]. The dataset is comprised of images of cells that were fluorescently stained against markers for DNA, beta-tubulin and F-actin. A subset of the captured images is labelled as the distinct MoA to represent phenotypic cell effects under drug treatments [17, 10].

Figure 2 shows the overview of the experiment. During the experiment, CP representations are obtained by feeding original BBBC021 cell images into CellProfiler software [16]. Every dimension in the CP representations describes an aspect of biological phenotypic information called a feature. The location of the nucleus centre in CP representations is used as the centre of single-cell images during segmentation. To be comparable with other work [5, 7, 14], we only keep the MoA annotated subset of 480k single-cell patches and their corresponding CP representations. Then we feed the single-cell images to the CP2Image model to generate images and evaluate the generating performance by comparing them with VAE and VAEplus models. To investigate which feature has been retained well in the generating process, we measure CP on generated images and original images, then calculate the pairwise correlation between these two measurements for different features.

3.2 Results

CP representations generate realistic cell images via CP2Image model: To explore the generative performance of CP2Image model, we generate images via CP2Image and compare them with images generated from VAE and VAEplus. Figure 3 shows four generated images from different models. To quantify the generating performance, we evaluate the images by FID score, with smaller values indicating greater similarity between generated images and real images. Table 3.2 illustrates that CP2Image model can generate less blurry cell images than VAE model, thus CP2Image has superior generative ability compared to the basic VAE. Even though CP2Image has a higher FID score than VAEplus, it should be noted that CP2Image only uses CP representation to produce images, whereas VAE and VAEplus both generate reconstructed images using original images. Figure 3 also indicates that generated images via the CP2Image model have similar nuclei compared to the original images; however, they could not reconstruct the shape of whole cells very well, where the boundaries are sometimes blurry or of irregular shape.

Correlating features from generated images with original images: To further explore if the generated images maintain biological phenotypic information, and which feature column in CP representations has been retained in the generating process, we calculate the pairwise correlation of CP measurement between the original and generated images. Figure 4(a) shows the correlation coefficient value, and we can see that more than 30% of feature dimensions have a correlation coefficient larger

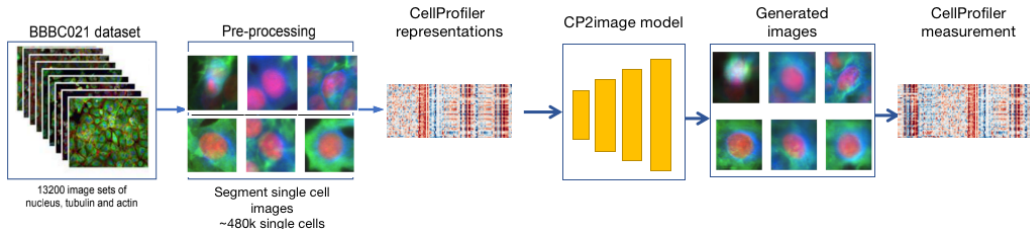


Figure 2: Overview of the experiment: segmentation of single cell images from data pre-processing, extraction of CP representations, images generation via CP2Image model, evaluation of generative performance and downstream analysis.

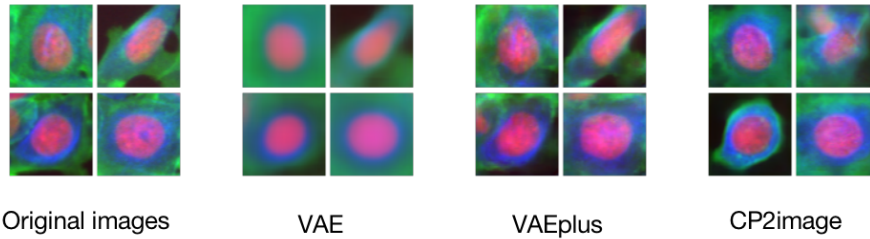


Figure 3: Comparison of original single-cell images and their corresponding images generated by VAE, VAEplus, and the proposed CP2Image model.

| | VAE | VAEplus | CP2Image |
|-----|------------------|-----------------|-----------------|
| FID | 351.96 ± 5.3 | 27.98 ± 3.8 | 68.42 ± 1.9 |

Table 1: FID is computed by comparing real images and images generated by different models. The average and standard deviation from three identical trials with random initialization are shown here.

than 0.5. These highly correlated features demonstrate a large amount of morphological information has been well-preserved during generating process. The 20 features with the largest value are about the shape and intensity of the nucleus, while those features with the smallest values are almost features which describe the distribution of intensity over the single-cell image. Figure 4(b) shows the 4 dimensions with the highest correlation coefficient values. Figure 4(c) demonstrates when we manipulate a single well-preserved interpretable dimension, the generated images show corresponding variation. For example, nuclear area feature measures the number of pixels in nuclei. When we increase its value and fix all other feature dimensions, from top to bottom, the size of the nucleus gradually increases. The nuclear orientation feature measures the angle between the horizontal axis and major axis of the nuclei ellipse. Increasing its value allows us to observe a clockwise orientation variation in the generated images.

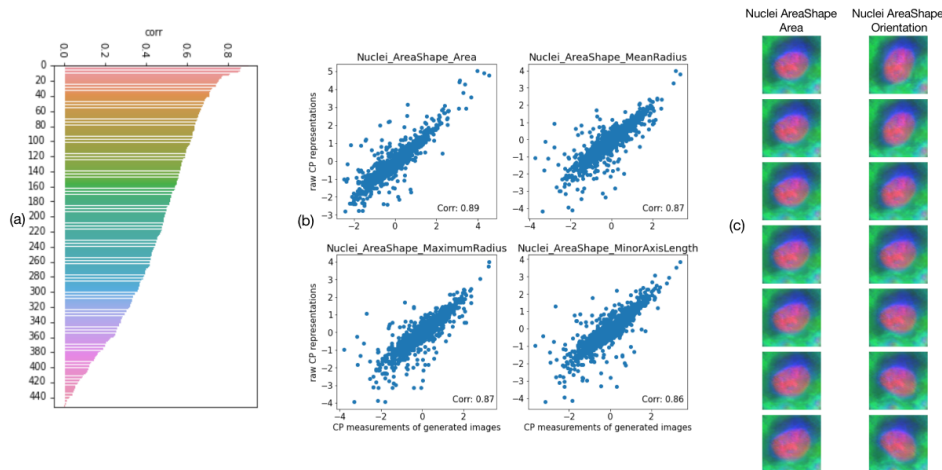


Figure 4: (a) Correlation between the original CP representations of single-cell patches and the CP representation of the CP2Image generated images. (b) Scatter plot of four dimensions of CP representation of single-cell patches and CP measurement with the highest correlation coefficient. (c) Manipulation of a single dimension in the CP representation; increase the value of the nucleus area feature (left) and nuclear orientation feature (right), respectively, and generate images from top to bottom. We note the clear change of nucleus size in the leftmost column going from top to bottom, and a change in orientation in the rightmost column, as expected.

4 Conclusion

In this work, we present the CP2Image model to generate high-quality, single-cell images from CP representations. We also show most biological information is well-preserved in the generated images and it is the first time that hand-crafted representations are shown to have the generative ability. Our work has potential practical usage. For example, emerging image-based drug screens often report only conventional descriptive computer vision features rather than actual images. Having the ability to turn these features into photo-realistic images gives scientists an intuitive way to compare their own images with large-scale reference datasets. Our work shows promising prospects in this field.

References

- [1] D Michael Ando, Cory Y McLean, and Marc Berndl. Improving phenotypic measurements in high-content imaging screens. *BioRxiv*, page 161422, 2017.
- [2] Juan C Caicedo, Claire McQuin, Allen Goodman, Shantanu Singh, and Anne E Carpenter. Weakly supervised learning of single-cell feature embeddings. In *Proceedings of the IEEE Conference on Computer Vision and Pattern Recognition*, pages 9309–9318, 2018.
- [3] Anne E Carpenter, Thouis R Jones, Michael R Lamprecht, Colin Clarke, In Han Kang, Ola Friman, David A Guertin, Joo Han Chang, Robert A Lindquist, Jason Moffat, et al. Cellprofiler: image analysis software for identifying and quantifying cell phenotypes. *Genome biology*, 7(10):1–11, 2006.
- [4] Peter Goldsborough, Nick Pawlowski, Juan C Caicedo, Shantanu Singh, and Anne E Carpenter. Cytogan: generative modeling of cell images. *BioRxiv*, page 227645, 2017.
- [5] Rens Janssens, Xian Zhang, Audrey Kauffmann, Antoine de Weck, and Eric Yves Durand. Fully unsupervised deep mode of action learning for phenotyping high-content cellular images. *bioRxiv*, 2020.
- [6] Diederik P Kingma and Max Welling. Auto-encoding variational bayes. *arXiv preprint arXiv:1312.6114*, 2013.
- [7] Maxime W Lafarge, Juan C Caicedo, Anne E Carpenter, Josien PW Pluim, Shantanu Singh, and Mitko Veta. Capturing single-cell phenotypic variation via unsupervised representation learning. In *International Conference on Medical Imaging with Deep Learning*, pages 315–325. PMLR, 2019.
- [8] Li Li, Wei-Yi Cheng, Benjamin S Glicksberg, Omri Gottesman, Ronald Tamler, Rong Chen, Erwin P Bottinger, and Joel T Dudley. Identification of type 2 diabetes subgroups through topological analysis of patient similarity. *Science translational medicine*, 7(311):311ra174–311ra174, 2015.
- [9] Maxwell W Libbrecht and William Stafford Noble. Machine learning applications in genetics and genomics. *Nature Reviews Genetics*, 16(6):321–332, 2015.
- [10] Vebjorn Ljosa, Peter D Caie, Rob Ter Horst, Katherine L Sokolnicki, Emma L Jenkins, Sandeep Daya, Mark E Roberts, Thouis R Jones, Shantanu Singh, Auguste Genovesio, et al. Comparison of methods for image-based profiling of cellular morphological responses to small-molecule treatment. *Journal of biomolecular screening*, 18(10):1321–1329, 2013.
- [11] Takeru Miyato, Toshiki Kataoka, Masanori Koyama, and Yuichi Yoshida. Spectral normalization for generative adversarial networks. *arXiv preprint arXiv:1802.05957*, 2018.
- [12] Nick Pawlowski, Juan C Caicedo, Shantanu Singh, Anne E Carpenter, and Amos Storkey. Automating morphological profiling with generic deep convolutional networks. *BioRxiv*, page 085118, 2016.
- [13] Gianluca Pegoraro and Tom Misteli. High-throughput imaging for the discovery of cellular mechanisms of disease. *Trends in Genetics*, 33(9):604–615, 2017.
- [14] Alexis Perakis, Ali Gorji, Samridhi Jain, Krishna Chaitanya, Simone Rizza, and Ender Konukoglu. Contrastive learning of single-cell phenotypic representations for treatment classification. *arXiv preprint arXiv:2103.16670*, 2021.
- [15] Wesley Wei Qian, Cassandra Xia, Subhashini Venugopalan, Arunachalam Narayanaswamy, Michelle Dimon, George W Ashdown, Jake Baum, Jian Peng, and D Michael Ando. Batch equalization with a generative adversarial network. *Bioinformatics*, 36(Supplement_2):i875–i883, 2020.
- [16] Shantanu Singh, M-A Bray, TR Jones, and AE Carpenter. Pipeline for illumination correction of images for high-throughput microscopy. *Journal of microscopy*, 256(3):231–236, 2014.

- [17] Matthew D Smith and Christopher V Maani. Mechanism of action. *Int. J. Clin. Pract. Suppl.*, 121:13–18, 2001.
- [18] Nicholas P Tatonetti, P Ye Patrick, Roxana Daneshjou, and Russ B Altman. Data-driven prediction of drug effects and interactions. *Science translational medicine*, 4(125):125ra31–125ra31, 2012.
- [19] Fei Wang, Ping Zhang, Xiang Wang, and Jianying Hu. Clinical risk prediction by exploring high-order feature correlations. In *AMIA Annual Symposium Proceedings*, volume 2014, page 1170. American Medical Informatics Association, 2014.
- [20] Roy Wollman and Nico Stuurman. High throughput microscopy: from raw images to discoveries. *Journal of cell science*, 120(21):3715–3722, 2007.